Formation of Phenoxy and Cyclopentadienyl Radicals from the Gas-Phase Pyrolysis of Phenol

Lavrent Khachatryan, Julien Adounkpe, and Barry Dellinger*

Louisiana State University, Baton Rouge, Louisiana 70803

Received: May 23, 2007; In Final Form: August 15, 2007

The formation of radicals from the gas-phase pyrolysis of phenol over a temperature range of 400−1000 °C was studied using the technique of low temperature matrix isolation electron paramagnetic resonance (LTMI EPR). Cooling the reactor effluent in a CO_2 carrier gas to 77 K produces a cryogenic matrix that exhibits complex EPR spectra. However, annealing by slowly raising the matrix temperature yielded well-resolved, identifiable spectra. All annealed spectra over the temperature range of 700−1000 °C resulted in the generation of EPR spectra with six lines, hyperfine splitting constant ∼6.0 G, $g = 2.00430$, and peak-to-peak width ∼3 G that was readily assignable, based on comparison with the literature and theoretical calculations, as that of cyclopentadienyl radical. Annihilation procedures along with microwave power saturation experiments helped to clearly identify phenoxy radicals in the same temperature region. Conclusive identifications of cyclopentadienyl and phenoxy radicals were based on pure spectra of these radicals under the same experimental conditions generated from suitable precursors. Cyclopentadienyl is clearly the dominant radical at temperatures above 700 °C and is observed at temperatures as low as 400 °C. The low-temperature formation is attributed to heterogeneous initiation of phenol decomposition under very low pressure conditions. The high cyclopentadienyl to phenoxy ratio was consistent with the results of reaction kinetic modeling calculations using the CHEMKIN kinetic package and a phenol pyrolysis model adapted from the literature.

1. Introduction

Phenol and substituted phenols play an important role in the combustion of aromatic compounds as they are typically the first oxidation product of an aromatic hydrocarbon.[1−3] Phenol is also a likely reaction intermediate in the decomposition of hydroquinones and catechols[1,3] that are formed in the combustion of tobacco and other biomass which are implicated as precursors in the formation of biologically active, semiquinone-type free radicals. Although the combustion and thermal degradation of phenol has been the topic of some research, its role in the formation of environmentally persistent free radicals (PFRs) has only recently begun to be explored.[4]

There are a few reports of the high-temperature (∼900−1200 K) pyrolysis of phenol. Generally the published results concern the nature of the initiation step. Some authors conclude that the hydroxylic hydrogen atom of the C_6H_5OH enol structure tautomerizes to form the C_6H_6O keto structure before decomposing into carbon dioxide and cyclopentadiene (C_5H_6),[5,6] with the cyclopentadienyl radical, C_5H_5 (CPD radical), then being formed from the cylcopentadiene molecule.[6] It has also been proposed that the initiation step of the phenol decay is the formation of phenoxy (C_6H_5O) + H followed by the phenoxy decomposition into CPD radical and carbon monoxide.[7−9]

At the present time, we are not aware of any published literature demonstrating direct experimental proof of formation of phenoxy or CPD radicals during phenol pyrolysis. Consequently, identification of the exact nature of the radicals from phenol pyrolysis, their origin, their stability, and the potential health impacts of possibly environmentally persistent free radicals appears to be an increasingly important environmental issue.

We have studied the thermal degradation of phenol under controlled conditions that allowed trapping of decomposition radical(s) under conditions that facilitated their identification. We employed the technique of low temperature matrix isolation (LTMI) EPR,[10] in which phenol was pyrolyzed in a low-pressure reactor (0.1−0.3 Torr) that was directly connected to a liquid nitrogen cooled cold finger situated within the EPR cavity of a Bruker EPR spectrometer. The experimental system was configured such that matrix isolation gases could be introduced to improve the quality of the resulting EPR spectra. In some experiments, gradual warming of the Dewar was employed to allow annealing of the matrix and annihilation of mobile or very reactive radicals. This resulted in production of cleaner, sharper spectra of single radicals under environmentally isolated conditions. These simple annealing experiments in conjunction with the LTMI EPR technique allowed the identification of phenoxy and CPD radicals in the complex mixture of radicals from pyrolysis of phenol over the surprisingly wide pyrolysis temperature range of 400−1000 °C.

2. Experimental Procedure

A technique referred to in the literature as low temperature matrix isolation EPR (LTMI EPR) was used in this study.[10−14] LTMI EPR allows accumulation and detection of trace quantities of radicals from the gas phase as well as the determination of the reaction kinetic behavior of gas-phase reactions. With the aid of this simple method, it is possible to follow the kinetic behavior of various radicals produced during the combustion of many classes of organic compounds.[10,15]

* Corresponding author. Telephone: (225) 578-6759. Fax: (225) 578-0276. E-mail: barryd@lsu.edu.

10.1021/jp073999m CCC: $40.75
Published on Web 12/23/2007

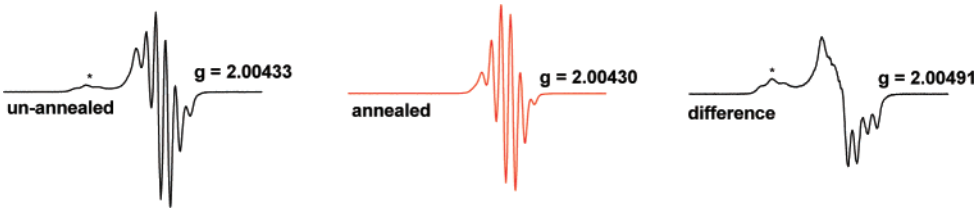

Figure 1. EPR spectra of carbon dioxide matrix isolated radicals from the pyrolysis of phenol at 950 °C before (unannealed spectrum, DI/N = 25.73) and after annealing (middle spectrum, DI/N = 12.4). The right-side spectrum is the difference spectrum (DI/N = 17.0). All spectra were registered at sweep width 200 G, modulation amplitude 4 G, time constant 5.12 ms, and microwave power 5 mW. The DI/N value is the double-integrated (DI) intensity of the EPR spectrum that has been normalized (N) to account for the conversion time, receiver gain, number of data points, and sweep width [http://www.bruker-biospin.com/winepr.html?&L=0]. The weak spectrum denoted by an asterisk has been reported to be due to cyclohexadienyl radicals formed by hydrogen addition to the aromatic ring of phenol.[19−21]

In our experiments, a thermoelectrically heated reactor was used for the pyrolysis of phenol. It was interfaced to a liquid nitrogen cooled Dewar located in the cavity of an EPR spectrometer which allows the detection and identification of radicals arising immediately during gas-phase pyrolysis (details in ref 16). Reagents are pumped by means of rotary pumps at a pressure of <0.3 Torr through the thermoelectrically heated pyrolysis zone. To maintain a constant delivery rate of phenol, a vaporizer held at 15 °C was used. The delivery rate of phenol was of 1.66×10^{-2} mmol/min (phenol concentration of 150 ppm) in a carrier gas of CO_2 at a flow rate of 12.12×10^{-2} mmol/min with a gas-phase residence time in the high-temperature portion of the reactor of 4 ms. The same carbon dioxide carrier gas was used as a supporting matrix to assist in the freezing of radicals. Pyrolysis products were condensed onto the cold finger of the Dewar placed in the EPR cavity and cooled by liquid nitrogen.

All EPR spectra were recorded on a Bruker EMX-20/2.7 EPR spectrometer (Bruker Instruments, Billerica, MA) with dual cavities, X-band, 100 kHz, and microwave frequency, 9.516 GHz. In most cases, the typical parameters were sweep width 200 G, EPR microwave power from 0.1 to 20 mW, modulation amplitude ≤4 G, constant time, and changeable sweep time. Values of *g*-factors were calculated using Bruker's WINEPR program.

Gradual warming of the Dewar resulted in annealing of the matrix and selective annihilation of the more reactive radicals such that the spectra of the more persistent, individual radicals in the mixture could be discerned. It is known that radical diffusion and resulting radical−radical recombination in cold matrixes occurs at a temperature well below the melting point of the matrix.[17] Usually the radicals begin to disappear when the temperature rises to between 1/10 and 1/3 of the melting point of the matrix (130−176 K). The cold finger of the Dewar was slowly warmed by removing liquid nitrogen with a bubbling stream of nitrogen gas resulting in some of the initially observed reactive radicals being annihilated by radical−radical recombination.

Gas-phase, room-temperature UV photolysis of phenol was used to generate phenoxy radical as an EPR standard under conditions where thermal degradation did not generate other radicals that interfered with structural assignments. In place of the pyrolysis reactor, we substituted a photolytic cell, a simple Suprasil 1 quartz tube, which was irradiated by 253.7 nm UV light from the side.[16] The 253.7 nm light was generated using a conventional, mercury vapor, ozone-free pencil lamp from Jelight, Inc. This double-bore lamp, with a 9 mm outside diameter, produced a 4 in. light at a power of ∼9 mW/cm^2 at 254 nm measured at a distance of 15 mm from the lamp.

3. Results and Discussion

The LTMI EPR technique, in spite of its many advantages, is limited in identification of trapped radicals when the observed EPR spectra arise from two or more species.[16] One of the principal EPR spectral identification parameters, the apparent *g*-value (as a maximum point of the integrated curve), does not convey conclusive structural information when the EPR spectrum is a convolution of two or more species. Constituent

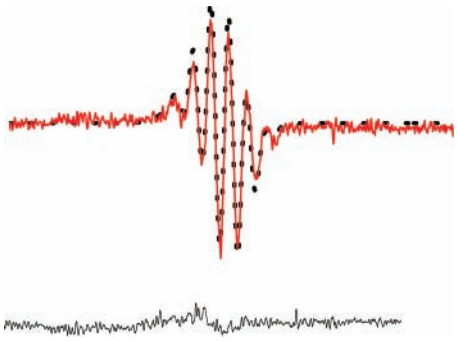

Figure 2. Comparison and subtraction of EPR spectra of carbon dioxide matrix isolated CPD radicals from the pyrolysis of η^5-C_5H_5-$Mn(CO)_3$ at 250 °C (upper spectrum, solid red line, $g = 2.00431$) with the annealed-residue spectrum of phenol pyrolysis at 950 °C (dotted black line, $g = 2.00430$). The lower trace is the difference spectrum. The spectra were registered at sweep width 150 G, modulation amplitude 4 G, time constant 5.12 ms, and microwave power 5 mW.

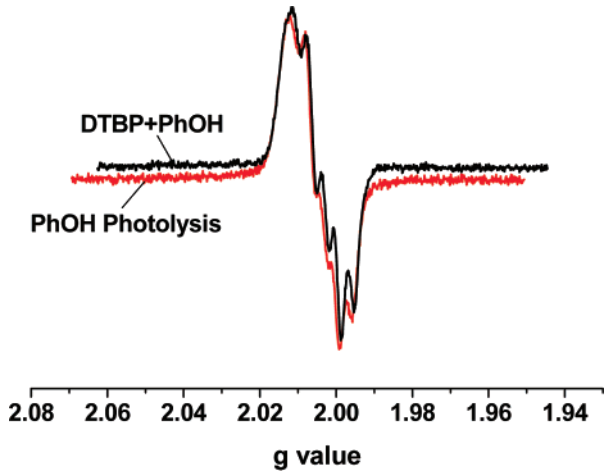

Figure 3. EPR spectra of phenoxy radicals at 77 K obtained using the LTMI EPR technique: red line, from phenol photolysis at 253.7 nm, $g = 2.00600$ in CO_2 matrix; black line, from thermolysis of DTBP + PhOH mixture at 250 °C in CO_2 flow; $g = 2.00582$. EPR parameters: sweep width, 200 G; modulation amplitude, 4 G; time constant, 40.96 ms; microwave power, 0.2 mW. At higher microwave powers (>2 mW) phenoxy radical EPR spectra were converted to a singlet line with apparent *g*-factors of 2.00480−2.00500.

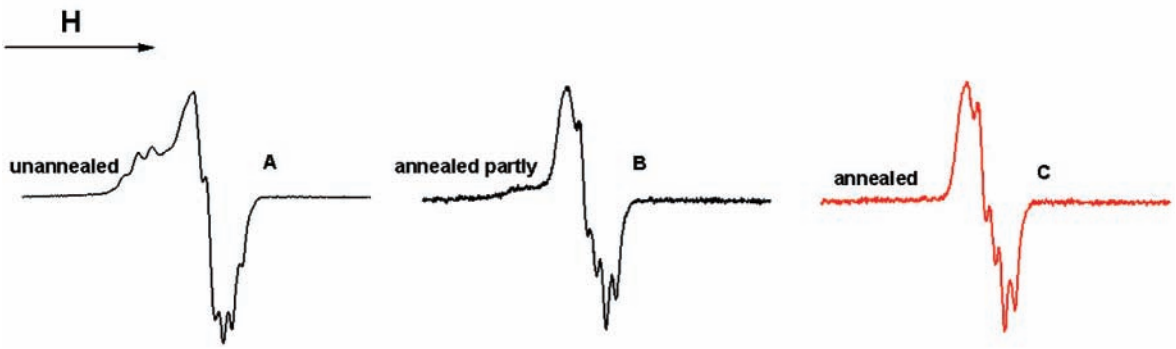

Figure 4. Step-by-step annihilation of initial spectrum A (g = 2.00745) to the final phenoxy radical spectrum C (g = 2.00582). EPR spectra registration conditions: sweep width, 200 G; modulation amplitude, 4 G; time constant, 5.12 ms; microwave power, 5 mW. The control reaction of 450 ppm of DTBP in a carbon dioxide flow produced a very weak anisotropic signal (data not shown).

radicals in a mixture can only be distinguished by judicious variation of the experimental conditions (temperature, pressure, annealing parameters, etc.) followed by computer analysis of digitally stored spectra. This procedure was used to simplify EPR spectra of gas-phase radicals trapped from phenol pyrolysis over the wide temperature region of 400−1000 °C.

Radicals from Pyrolysis of Phenol from 800 to 1000 °C. The 77 K EPR spectra from phenol pyrolysis at 950 °C, before and after annealing (cf. Figure 1), are similar to the previously reported spectra from the gas-phase pyrolysis of phenol at 750 °C.[16] A spectrum, tentatively identified as that of CPD radical, with six equidistant peaks and a center-line g-value of 2.00430 and $\Delta H_{p-p} \sim 3.0-3.1$ G was identified in the EPR spectrum of the annealed matrix (cf. Figure 1). The spectrum labeled "difference" in Figure 1 is the difference between unannealed and annealed spectra as represented by a simple subtraction using Simfonia software [http://www.bruker-biospin.com/simfonia.html]. Such mathematical manipulations are allowable if the radicals are trapped in a dilute matrix where the ratio of the gas-matrix flow to the pyrolysis gas flow is >10 as in our case.[11,15] Under these conditions, the mutual interaction of radicals can be avoided and the effect of the matrix on the shape of spectra can be also minimized.[18]

Approximately half the initial radicals disappeared during annealing, leaving behind the resolved, symmetrical, annealed spectrum. Subtraction of the annealed from the unannealed spectrum gave a difference spectrum that appeared to be a complex mixture of radicals. To identify the radicals evident in the unannealed and difference spectra, we separately generated pure CPD and phenoxy (PhO•) radicals from different precursors using various methods.

Comparison with CPD Radicals from Low-Temperature Pyrolysis of Tricarbonylcyclopentadienylmanganese (η^5-$C_5H_5Mn(CO)_3$) at 250 °C. The mechanism of the gas-phase pyrolysis of η^5-$C_5H_5Mn(CO)_3$ has been thoroughly investigated[22] using conventional and IR laser powered homogeneous pyrolysis in combination with matrix isolation EPR spectroscopy. The decomposition was consistent with initial stepwise loss of CO, followed ultimately by release of CPD radical.

We generated CPD radicals from pyrolysis of η^5-$C_5H_5Mn(CO)_3$ in a CO_2 gas flow at less than 0.2 Torr total pressure. The spectrum exhibits an isotropic 1:5:10:10:5:1 sextet (cf. red spectrum in Figure 2). The EPR spectrum of these radicals were compared and subtracted from the annealed EPR spectrum of phenol pyrolysis products at 950 °C (cf. Figure 2, dotted black line). Clearly the spectra are in excellent agreement, and the difference spectrum presented in the lower trace indicates that very few other radicals were present after annealing.

Based on comparison of the unannealed and annealed spectra in Figure 1, we can state that CPD radical comprises at least 50% of the radicals in the unannealed EPR spectrum. The other 50% may be a mixture of CPD, phenoxy, phenyl, and other unknown radicals. To confirm the presence of phenoxy radicals, we generated pure phenoxy radicals from the gas-phase photolysis of phenol as well as from the reaction of phenol with the radicals from di-*tert*-butyl peroxide (DTBP) pyrolysis.

Comparison to Phenoxy Radicals from Photolysis of Phenol and the Low-Pressure, Gas-Phase Reaction of DTBP (Di-tert-butyl Peroxide) with Phenol. It is known that 250−300 nm photoexcitation of phenol in solution results in partial photodissociation to phenoxy radical and a hydrogen atom.[21,23,24] The EPR spectrum from the room-temperature, low-pressure photolysis of phenol vapor in CO_2 flow (total pressure ~0.2 Torr) using the LTMI EPR technique is depicted by the red line in Figure 3. This broad spectrum consists of five lines with apparent g = 2.00600 at 77 K in a carbon dioxide matrix and microwave power 0.202 mW. A very complex spectrum, 15 or more lines, of phenoxy radicals has been reported in liquid media.[25−27]

Di-*tert*-butyl peroxide (DTBP) was also used to generate phenoxy radicals through reacting the radicals produced by its decomposition with phenol:[28−30]

$$\text{DTBP} \rightarrow 2\ t\text{-BuO}^{\bullet} \quad \text{(I)}$$

$$t\text{-BuO} \rightarrow \text{Me} + \text{Me}_2\text{CO} \quad \text{(II)}$$

$$t\text{-BuO} + \text{RH(PhOH)} \rightarrow t\text{-BuOH} + \text{R}^{\bullet}\text{(PhO}^{\bullet}\text{)} \quad \text{(III)}$$

Accordingly, we pyrolyzed a mixture of 450 ppm DTBP and 250 ppm phenol at 250 °C in a flow of carbon dioxide (~0.3 Torr). The EPR spectra at 77 K of the pyrolysis products are depicted in Figure 4 as well as in Figure 3. Step-by-step annealing of the matrix converted the unannealed spectrum A (g = 2.00745) to intermediate spectrum B (g = 2.00607) and the fully annealed spectrum C (g = 2.00582), which matches exactly the spectrum of the photochemically generated phenol (cf. Figure 3).

Due to the small difference in the components of the g-tensors for phenoxy radicals, an anisotropic spectral analysis is impossible on the X-band because many anisotropic peaks overlap.[31] The single characteristic parameter in our case is the high g-value (2.00482−2.00500 at high microwave power, >2 mW) which is in the range of the g-values for phenoxy radicals in liquid solution (~2.00461) and substituted phenoxy radicals (non-halogenated) in various media of ~2.00530 (Table 1). This shift of the g-value depends significantly on the spin density of

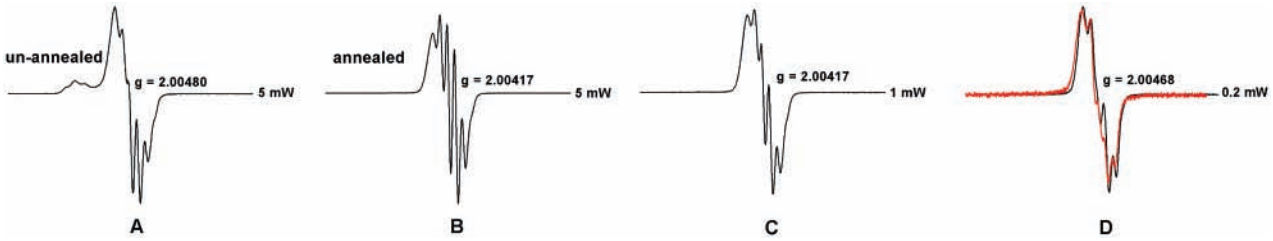

Figure 5. EPR spectra of frozen radicals (at 77 K) from phenol pyrolysis at 950 °C. Spectrum A, initial spectrum at 5 mW power. Spectrum B, after annealing at 5 mW power. Spectrum C, annealed spectrum at 1 mW. Spectrum D, annealed spectrum at 0.2 mW (black line) overlaid with the spectrum of pure phenoxy (red line) recorded under the same conditions (from phenol photolysis at 0.2 mW power).

TABLE 1: EPR Spectral Characteristics of Phenoxy and Substituted Phenoxy Radicals

radical	*T*	no. of lines	*g*, center	hfsc,[a] G	ref
phenoxy[b]	room temp	15 lines	NA	6.6 ortho 1.85 meta 10.22 para	25
phenoxy[c]	room temp	multilines	2.00461	6.61 ortho 1.85 meta 10.22 para	26
phenoxy/bulk[d]	room temp	poorly resolved singlet	2.00450	–	37
phenoxy[e]	room temp	multilines	2.00530	7.01 2.05 10.13	27
phenoxy[f]	123 K	anisotropic, broad, three lines	2.00539	1.54 meta 2.66 para[g]	31
p-Cl-phenoxy[h]	room temp	14	2.00630	6.56, 1.99	27

[a] hfsc, hyperfine splitting constant. [b] Phenol aqueous solution, oxidation by ceric sulfate; NA, not available in the original source. [c] Phenol aqueous solution, radiolysis. [d] Polyradical, in benzene, poly(phenylenevinylene)-attached phenoxy radicals. [e] Phenol in CCl_4, photooxidation. [f] Produced from α-(3,5-di-*tert*-butyl-4-hydroxyphenyl)-*N*-*tert*-butylnitrone by oxidation (PbO_2) in toluene. [g] $N_\perp = 1.57$; $N_\parallel = 12.35$. [h] *p*-Cl-phenol in CCl_4, photooxidation.

the phenolic oxygen, ρ_o^π. Theoretical and experimental studies of model compounds suggest that there is a positive, direct proportionality between ρ_o^π and the *g*-value.[32,33] The presence of a hydrogen bond to the oxygen reduces ρ_o^π and, consequently, the *g*-factor.[34,35] As a result, hydrogen bonding in aqueous solution results in the somewhat lower *g*-factor of 2.004 61[36] while higher *g*-values of ~2.00530 are observed in more nonpolar solvents such as CCl_4[27] (Table 1).

We performed additional experiments to determine if phenoxy radical was generated by pyrolyzing phenol without carrier gas. The reason for this is that if CPD/phenoxy radicals are not diluted by CO_2, then based on their differing stability/reactivity behavior (section 4.0) they may partially dimerize and result in simpler, more interpretable EPR spectra. In the absence of CO_2 the spectrum (cf. Figure 5, spectrum A) resembles the residue (difference) spectrum in Figure 1. Annealing converted spectrum A (DI/N = 24.18) to the much better resolved spectrum B (DI/N = 11.07) and finally spectrum C (DI/N = 8.00). Decreasing the microwave power to 0.2 mW resulted in spectrum D (black line, DI/N = 3.7, $g = 2.00468$). This residue spectrum matches very well the EPR spectrum of pure phenoxy radical (overlaid at the same *g*-value scale, red line in spectrum D). Thus, the combination of performing the experiments without a matrix and with annealing promotes CPD/phenoxy radical destruction at different rates, which, along with reducing the microwave power, enhances the spectrum of phenoxy over that of CPD radical such that it can be clearly resolved (vide infra, Figure 7). All these procedures result in a residue spectrum (Figure 5D) nearly identical to that of phenoxy and confirming its formation from pyrolysis of phenol from 800 to 1000 °C.

Radicals from Pyrolysis of Phenol from 700 to 800 °C. The EPR spectrum in this region is similar to the high-temperature pyrolysis spectra, but with somewhat altered spectral intensities. Using the observation that increasing the microwave power readily saturates the EPR spectrum of phenoxy radicals but not CPD radicals,[16,38] we performed a series of phenol pyrolysis experiments from 700 to 800 °C to further investigate the nature of the radicals in the mixture.

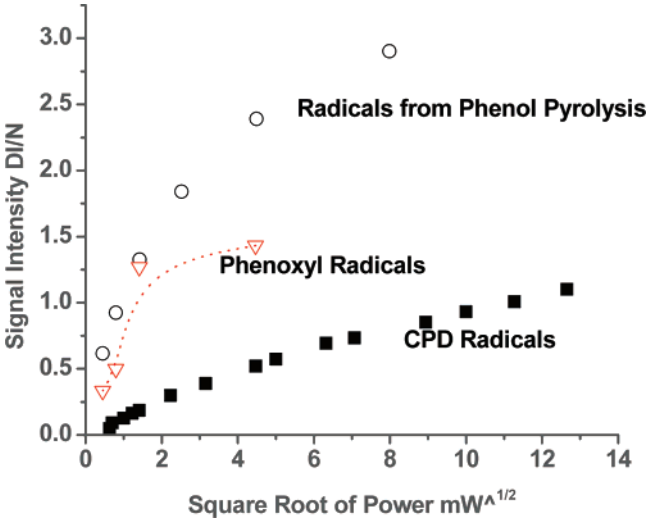

Figure 6. Microwave power dependence of CPD radicals at 77 K from pyrolysis of η^5-$C_5H_5Mn(CO)_3$ at 250 °C (squares), radicals from phenol pyrolysis at 700 °C (circles), and phenol photolysis (triangles).

Microwave Power Dependence. The power dependence of EPR spectra of radicals at 77 K from phenol pyrolysis at 700 °C, phenol photolysis at room temperature, and CPD radicals from η^5-$C_5H_5Mn(CO)_3$ pyrolysis at 250 °C is presented in Figure 6.

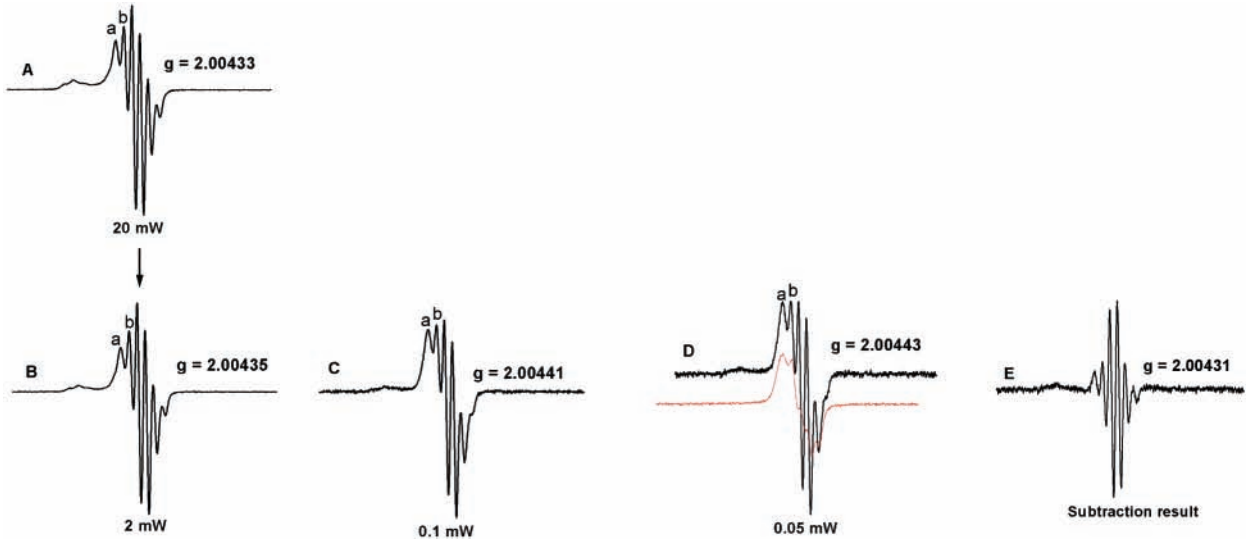

Figure 7. (A−D) Spectra depicting the effect of microwave power on the 77 K EPR spectra of radicals from the pyrolysis of phenol at 750 °C. Overlaid in red in spectrum D is the EPR spectrum of pure phenoxy radical. The peaks labeled "a" and "b" are the most dependent on microwave power. Subtraction of the spectrum of pure phenoxy radical from spectrum D results in the residue spectrum E, which is characteristic of CPD radical.

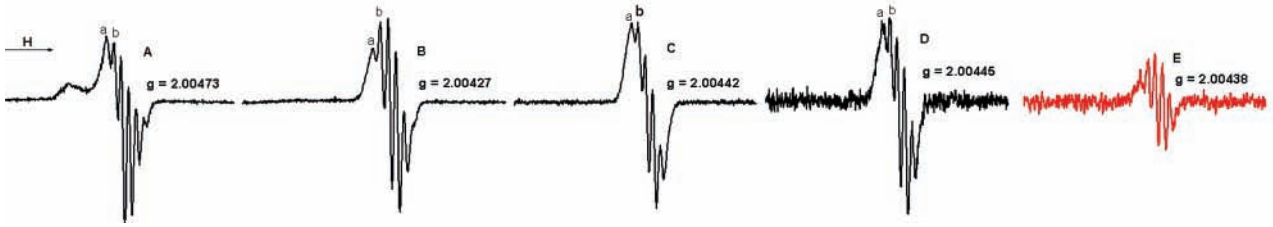

Figure 8. Step-by-step annealing of radicals from pyrolysis of phenol at 700 °C. All spectra were registered at the same conditions (sweep width, 200 G; modulation amplitude, 4 G; microwave power, 20 mW; time constant, 5.12 ms).

CPD radical spectra were observable up to microwave powers of 36−40 mW with insignificant saturation occurring at powers even greater than 40 mW. CPD radical spectra did not change in shape or intensity distribution over the entire region, which is consistent with reports in the literature,[38] while pure phenoxy radicals saturated easily at less than ∼1.5 mW (triangles, dotted line in Figure 6). It is also evident from Figure 6 that the magnetic susceptibility of phenoxy radicals at microwave powers less than 2 mW is significantly higher than that of CPD radicals while at higher power this is reversed. If we assume a mixture of these two radicals, we would expect an intermediate saturation behavior of this mixture as is the case of the EPR spectra from the pyrolysis of phenol (cf. Figure 6, circles), which begins to saturate at powers less than 10 mW.

The large magnetic susceptibility of CPD radicals at high power (20 mW) causes the EPR spectra resulting from the pyrolysis of phenol (cf. spectrum A in Figure 7) to be dominated by the CPD radical spectrum. Decreasing the power results in relative growth of two peaks marked "a" and "b" that resemble those of phenoxy radicals (compared with overlaid spectra of pure phenoxy radical, red line in spectrum D). Subtraction of the EPR spectrum of phenoxy from spectrum D results in spectrum E, which clearly resembles that of CPD radical. This is additional evidence of the existence of phenoxy and CPD radicals from phenol pyrolysis at 750 °C.

Phenoxy Radicals in Step-by-Step Annealing Experiments. The 77 K EPR spectra of radicals from the pyrolysis of phenol at 700 °C are depicted in Figure 8 following stepwise annealing.

Intermediate annealing in spectra C and D clearly display peaks a and b, which are characteristic of phenoxy radical. Further annealing leads to annihilation of both phenoxy and CPD radicals and finally EPR spectra that perfectly match the spectrum of pure CPD radical from η^5-$C_5H_5Mn(CO)_3$ pyrolysis. The DI/N value varied from 2.337 (spectrum A) to 0.063 for nearly pure CPD radicals (spectrum E). (The initial concentration

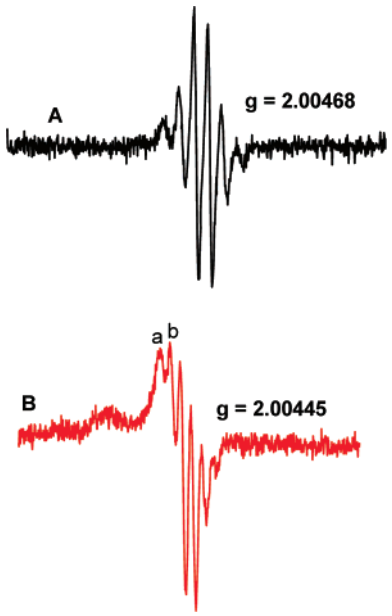

Figure 9. 77 K EPR spectra of radicals from pyrolysis of phenol in CO_2 flow at 400 °C (spectrum A) and at 600 °C (spectrum B). Registration parameters, spectrum A: sweep width, 200 G; modulation amplitude, 2 G; time constant, 20.48 ms; microwave power, 2 mW; five scans. Spectrum B: sweep width, 200 G; modulation amplitude, 4 G; time constant, 5.12 ms; microwave power, 2 mW; one scan.

TABLE 2: Reaction Kinetic Model for the Pyrolysis of Phenol (from Ref 6)[a]

	reactions considered	*A*	*b*	*E*
1	$C_6H_5OH = C_5H_6 + CO$	1.00×10^{12}	0.0	60 740.0
2	$C_6H_5OH = C_6H_5O + H$	3.20×10^{15}	0.0	81 500.0
3	$C_6H_5OH + H = C_6H_6 + OH$	2.20×10^{13}	0.0	8 000.0
4	$C_6H_5OH + H = C_6H_5O + H_2$	1.15×10^{14}	0.0	12 400.0
5	$C_6H_5OH + H = C_6H_5O + H_2O$	6.00×10^{14}	0.0	0.0
6	$C_6H_5O = C_5H_5 + CO$	7.40×10^{11}	0.0	43 800.0
7	$C_5H_6 = C_5H_5 + H$	4.00×10^{14}	0.0	77 000.0
8	$C_5H_6 + H = C_5H_5 + H_2$	2.80×10^{13}	0.0	2 260.0
9	$C_5H_6 + H = C_3H_5 + C_2H_2$	6.60×10^{14}	0.0	12 310.0
10	$C_5H_5 = C_5H_5(L)$	7.50×10^{11}	1.0	77 000.0
11	$C_5H_5(L) = C_3H_3 + C_2H_2$	3.70×10^{11}	0.0	30 000.0
12	$2C_5H_5 = C_{10}H_8 + 2H$	2.00×10^{13}	0.0	4 000.0
13	$2C_3H_3 = C_6H_5 + H$	1.00×10^{13}	0.0	0.0
14	$C_3H_3 + H = C_3H_4$	5.00×10^{13}	0.0	0.0
15	$C_3H_4 + H = C_3H_3 + H_2$	5.00×10^{7}	2.0	5 000.0
16	$C_3H_4 + H = CH_3 + C_2H_2$	1.00×10^{14}	0.0	4 000.0
17	$C_6H_5 = C_6H_5(L)$	2.50×10^{13}	0.0	70 500.0
18	$C_6H_5(L) = C_4H_3 + C_2H_2$	7.90×10^{62}	−14.7	57 000.0
19	$C_4H_3 = C_4H_2 + H$	1.60×10^{43}	−9.3	43 100.0

[a] *A* is in units of mol·cm·s·K; *E* is in units of cal/mol. $k = AT^b \exp(-E/RT)$.

TABLE 3: CPD Radical and Phenoxy Concentrations (Molar Ratio) from the Phenol Reaction Kinetic Model

	873 K	973 K	1073 K	1173 K	1273 K
C_5H_5	0.64×10^{-10}	0.80×10^{-7}	0.12×10^{-4}	0.36×10^{-3}	0.38×10^{-2}
C_6H_5O	0.28×10^{-8}	0.28×10^{-6}	0.48×10^{-5}	0.18×10^{-4}	0.43×10^{-4}
C_5H_5/C_6H_5O	0.023	0.3	2.5	19.7	88.4
percent consumption of C_6H_5OH	0.0	2.0	2.4	4.0	26.0

of radicals decreased by a factor of 40 from spectrum A to spectrum E as the matrix was annealed, and CPD radicals were still readily detectable.) This observation suggests that CPD radicals are in higher concentration than phenoxy radicals in the initial radical mixture and more CPD radicals survive after annealing and annihilation. Thus, in this temperature range, the pyrolysis of phenol produces both phenoxy and CPD radicals, with CPD being the dominant radical.

Radicals from Pyrolysis of Phenol from 400 to 700 °C. At 400 °C, the pyrolysis of phenol yielded a weak EPR signal that was clearly identifiable as CPD radical (cf. Figure 9A). The high activation barrier for CPD radical formation from elimination of CO from phenoxy radical (44−52 kcal/mol) would seem to preclude formation via a gas-phase reaction.[39−41] Consequently, the formation of CPD radical is attributed to a wall reaction. At a contact time of ∼4 ms and pressure of 0.2 Torr (reactor diameter ∼12 mm), the calculated diffusion time of a gas-phase phenol molecule to the quartz wall is only ∼70 μs, which means that the phenol molecules can collide with the wall almost 60 times prior to exiting the reaction zone.

The fact that we did not observe characteristic peaks for phenoxy radical at 400 °C suggests that the wall reaction of phenol proceeds directly to CPD radical without forming phenoxy radical as a stable intermediate. Surface-induced decomposition of phenol has been reported as low as 125 K through rupture of C_6H_5O-H bonds.[42] In this work, a surface reaction mechanism on Pt(III) was developed in which surface-adsorbed C_5H_3 and H_2 (or C_5H_5; the authors could not distinguish these products) were formed. Increasing the temperature to 600 °C accelerates the homogeneous gas-phase formation of phenoxy radicals, resulting in the characteristic peaks of the phenoxy radical labeled a and b depicted in Figure 9B.

Phenoxy and CPD Radical Yields. The high CPD radical to phenoxy radical ratio was a bit surprising in light of the stability of phenoxy radical proposed in the literature.[8,43] To address this question using our experimental results, we have modeled our experimental data with a core phenol pyrolysis model from the literature[6] using the CHEMKIN kinetic package[44] and a perfectly stirred, plug-flow reactor application (150 ppm phenol in flow of CO_2, total flow pressure 0.2 Torr, contact time 4 ms). The reaction kinetic input file was that proposed by Horn[6] without any changes in the kinetic parameters (cf. Table 2).

Examination of the results in Table 3 indicates that the C_5H_5 to C_6H_5O ratio is >1 above 1073 K and CPD radical increasingly dominates as the temperature increases.

Based on this model, phenoxy radical concentrations are most sensitive to the rates of reactions 2 and reaction 6. Reactions 4, 3, and 5 affect its concentration to a lesser degree in the order given. The CPD radical concentration is most sensitive to reaction 2 with lesser sensitivity to reactions 6, 4, 3, and 1, in that order.

The high CPD radical to phenoxy radical ratio can be understood if we analyze closely the results of the scheme in Table 2.

1. The relation $k_2 = 0.15k_1$ was necessary to explain the experimental yields of hydrogen atoms at very short times (∼200 μs) for the pyrolysis of phenol in shock-tube experiments according to ref 6. This results in a significant contribution to CPD radical formation through reactions 1 and 8.

2. Phenoxy radicals are actively decomposed to CPD radical at a higher rate (reaction 6) than CPD radical is decomposed to olefinic products (reactions 10 and 11).

3. The generation of radicals in chain propagation reactions also favors CPD radical (reaction 8) over phenoxy (reaction 4) because [H] ≫ [OH],[6] and formation of phenoxy through the well-known reaction $C_6H_5OH + OH = C_6H_5O + H_2O$ is depressed.

These factors result in CPD radical being the dominant PFR at temperatures >973 K. Below 973 K, the modeling calculation does not result in any conversion of phenol to CPD radical. However, because we have experimentally demonstrated the existence of CPD radicals at temperatures <973 that is not

predicted by the model, formation of CPD radical by wall reactions is implicated.

Insertion of a pathway for dimerization of phenoxy radicals (reactions 20 and 21)[45] did not change significantly the ratio of C_5H_5 to C_6H_5O, probably due to the low steady-state concentration of phenoxy radicals at 1173 K.

$$2C_6H_5O^{\bullet} \rightarrow C_{12}H_{10}O_2$$
$$k_{20} = 8.64 \times 10^{11} \exp(1254.0 \text{ cal/mol}/RT) \quad (20)$$

$$C_{12}H_{10}O_2 \rightarrow 2C_6H_5O$$
$$k_{21} = 3.16 \times 10^{15} \exp(-51000.0 \text{ cal/mol}/RT) \quad (21)$$

The rate of dimerization reaction of CPD radical, $k_{12} = 2.00 \times 10^{13} \exp(-4000 \text{ cal/mol}/RT)$ cm^3/mol·s, is comparable to the dimerization reaction of phenoxy radicals, $k_{20} = 8.6 \times 10^{11} \exp(1254 \text{ cal/mol}/RT)$ [46] (i.e., $k_{12}/k_{20} \sim 1.3$ at 700 K and ~3 at 1000 K).

All of these factors lead to CPD radicals being the dominant PFR over phenoxy radicals under low-pressure conditions.

Conclusions

We have studied the thermal degradation of phenol using the technique of low temperature matrix isolation (LTMI) EPR.[10] Phenol was pyrolyzed in a low-pressure reactor (0.1−0.3 Torr) that was directly connected to a liquid nitrogen cooled cold finger situated within the EPR cavity of a Bruker EPR spectrometer. The simple annealing experiments of the cold matrix as well as generation of pure radicals from suitable precursors and the different behaviors of microwave saturation curves of certain radicals allowed the identification of phenoxy and cyclopentadienyl radicals in the complex mixture of radicals from pyrolysis of phenol over the surprisingly wide pyrolysis temperature range of 400−1000 °C. Cyclopentadienyl is clearly the dominant radical at temperatures above 700 °C and is observed at temperatures as low as 400 °C. The low-temperature formation of cyclopentadienyl radical is attributed to heterogeneous initiation of phenol decomposition under very low pressure conditions. The high cyclopentadienyl to phenoxy ratio was consistent with the results of reaction kinetic modeling calculations using the CHEMKIN kinetic package and a phenol pyrolysis model adapted from the literature.

Acknowledgment. The authors gratefully acknowledge the partial support of this research by NSF (Grant CTS-0317094) and Philip Morris USA.

References and Notes

(1) Sakai, T.; Hattori, M. *Chem. Lett.* **1976**, 1153.
(2) Herring, A. M.; Kinnon, J. T.; Petrick, D. E.; Gneshin, K. W.; Filley, J. A.; McCloskey, B. D. *J. Anal. Appl. Pyrolysis* **2003**, *66*, 165.
(3) Marsh, N. D.; Ledesma, E. B.; Sandrowitz, A. K.; Wornat, M. J. *Energy Fuels* **2004**, *18* (1), 209.
(4) Dellinger, B.; Lomnicki, S.; Khachatryan, L.; Maskos, Z.; Hall, R. W.; Adunkpe, J.; McFerrin, C.; Truong., H. *31st International Symposium on Combustion, ScienceDirect, Proceedings of Combustion Institute, Elsevier, Pittsburgh, PA*; 2007; p 521.
(5) Cypres, R.; Bettens, B. *Tetrahedron* **1975**, *31*, 359.
(6) Horn, C.; Roy, K.; Frank, P.; Just, T. *27th Symposium (International) on Combustion/The Combustion Institute, Elsevier, Pittsburgh, PA*; 1998; p 321.
(7) Lovell, A. B.; Brezinsky, K.; Glassman, I. *Int. J. Chem. Kinet.* **1989**, *21*, 547.
(8) Manion, J. A.; Louw, R. *J. Phys. Chem.* **1989**, *93*, 3563.
(9) Brezinsky, K.; Pecullan, M.; Glassman, I. *J. Phys. Chem. A* **1998**, *102*, 8614.
(10) Nalbandyan, A. B.; Mantashyan, A. H. *The elementary processes in slow gas-phase reactions*; Inst. Chem. Phys. NA of Armenia; Yerevan, 1975.
(11) Khachatryan, L.; Niazyan, O.; Mantashyan, A. H.; Vedeneev, V. I.; Teitel'boim, M. A. *Int. J. Chem. Kinet.* **1982**, *14*, 1231.
(12) Carlier, M.; Pauwels, J. P.; Sochet, L.-R. *Oxid. Commun.* **1984**, *6*, 141.
(13) Davidson, I. M. T.; Ellis, A. M.; Mills, G. P.; Pennington, M.; Povey, I. M.; Raynor, J. B.; Russell, D. K.; Saydam, S.; Workman, A. D. *J. Mater. Chem.* **1994**, *4*, 13.
(14) Mach, K.; Mills, G. P.; Raynor, J. B. *J. Organomet. Chem.* **1997**, *532*, 229.
(15) Mantashyan, A. A.; Khachatryan, L. A.; Niazyan, O. M.; Arsentiev, S. D. *Combust. Flame* **1981**, *43*, 221.
(16) Khachatryan, L.; Adounkpe, J.; Maskos, M.; Dellinger, B. *Environ. Sci. Technol.* **2006**, *40*, 5071.
(17) Mile, B. *Angew. Chem., Int. Ed.* **1968**, *7*, 507.
(18) Aruthunyan, A. Z.; Grigoryan, G. L.; Nalbandyan, A. B. *Kinet. Katal.* **1986**, *27*, 1352.
(19) Ohnishi, S.-I.; Nitta, I. *J. Chem. Phys.* **1963**, *39*, 2848.
(20) Liebling, G. R.; McConnel, H. M. *J. Chem. Phys.* **1965**, *42*, 3931.
(21) Bussandri, A.; van Willigen, H. *J. Chem. Phys.* **2002**, *106*, 1524.
(22) Russell, D. K.; Davidson, I. M. T.; Ellis, A. M.; Mills, G. P.; Pennington, M.; Povey, I. M.; Raynor, J. B.; Saydam, S.; Workman, A. D. *Organometallics* **1995**, *14*, 3717.
(23) Jeevarajan, A. S.; Fessenden, R. W. *J. Chem. Phys.* **1992**, *96*, 1520.
(24) Bussandri, A.; van Willigen, H. *J. Phys. Chem.* **2001**, *105*, 4669.
(25) Stone, T. J.; Waters, W. A. *Proc. Chem. Soc., London* **1962**, 253.
(26) Neta, P.; Fessenden, R. W. *J. Phys. Chem.* **1974**, *78*, 523.
(27) Graf, F.; Loth, K.; Gunthard, H.-H. *Helv. Chim. Acta* **1977**, *60*, 710.
(28) Batt, L.; Benson, S. W. *J. Chem. Phys.* **1962**, *36*, 895.
(29) Mulcahy, M. F. R.; Williams, D. J.; Wilmshurst, J. R. *Aust. J. Chem.* **1964**, *17*, 1329.
(30) Yip, C. K.; Pritchard, H. O. *Can. J. Chem.* **1971**, *49*, 2290.
(31) Yamaji, T.; Noda, Y.; Yamauchi, S.; Yamauchi, J. *J. Phys. Chem. A* **2006**, *110*, 1196.
(32) Prabhananda, B. S. *J. Chem. Phys.* **1983**, *59*, 2509.
(33) Felix, C. C.; Prabhananda, B. S. *J. Phys. Chem.* **1984**, *80*, 3078.
(34) Burghaus, O.; Plato, M.; Rohrer, M.; Mobius, K.; MacMillan, F.; Lubitz, W. *J. Phys. Chem.* **1993**, *97*, 7639.
(35) Feber, G.; Isaacson, R. A.; Okamura, M. Y.; Lubitz, W. *Springer Ser. Chem. Phys.* **1985**, *42*, 174−189.
(36) Un, S.; Tang, X.-S.; Diner, B. A. *Biochemistry* **1996**, *35*, 679.
(37) Nishide, H.; Kaneko, T.; Nii, T.; Katoh, K.; Tsuchida, E.; Lahti, P. M. *J. Am. Chem. Soc.* **1996**, *118*, 9695.
(38) Barker, P. J.; Davies, A. G.; Tse, M.-W. *J. Chem. Soc., Perkin Trans.* **1980**, 2, 941.
(39) *NIST Chemical Kinetics Database 17*; Gaithersburg, MD, 1998.
(40) Collussi, A. J.; Zabel, F.; Benson, S. W. *Int. J. Chem. Kinet.* **1977**, *9*, 161.
(41) Liu, R.; Morokuma, K.; Mebel, A. M.; Lin, M. C. *J. Phys. Chem.* **1996**, *100*, 9314.
(42) Ihm, H.; White, J. M. *J. Phys. Chem. B* **2000**, *104*, 6202.
(43) McFerrin, C. A.; Hall, R. W.; Dellinger, B. Accepted for publication in *THEOCHEM* **2007**.
(44) Kee, R. J.; Rupley, F. M.; Miller, J. A.; Coltrin, M. E.; Grcar, J. F.; Meeks, E.; Moffat, H. K.; Lutz, A. E.; Dixon-Lewis, G.; Smooke, M. D.; Warnatz, J.; Evans, G. H.; Larson, R. S.; Mitchell, R. E.; Petzold, L. R.; Reynolds, W. C.; Caracotsios, M.; Stewart, W. E.; Glaborg, P.; Wang, C.; Adigun, O.; Houf, W. G.; Chou, C. P.; Miller, S. F. *CHEMKIN, Reaction Design*; San Diego, CA, 2002.
(45) Khachatryan, L. A.; Burcat, A.; Dellinger, B. *Combust. Flame* **2003**, *132*, 406.
(46) Berho, F.; Lesclaux, R. *Chem. Phys. Lett.* **1997**, *279*, 289.